Materials Science and Engineering C 77 (2017) 912–919

Contents lists available at ScienceDirect

Materials Science and Engineering C

journal homepage: www.elsevier.com/locate/msec

In vitro and in vivo evaluation of electrospun membranes of poly (ε-caprolactone) and poly (rotaxane)

Tais Helena Costa Salles [a], Daniel Isaac Sendyk [b], Natacha Kalline de Oliveira [b], Daisy Machado [c], Marcelo Lancellotti [c], Maria Cristina Zindel Deboni [b], Chang Tien Kiang [d], Marcos Akira d'Ávila [a,*]

[a] Department of Manufacturing and Materials Engineering, School of Mechanical Engineering, University of Campinas, Campinas, Brazil
[b] Department of Oral and Maxillofacial Surgery, Faculty of Dentistry, University of São Paulo, São Paulo, Brazil
[c] Laboratory of Biotechnology, Institute of Biology, University of Campinas, Campinas, Brazil
[d] Chemistry and Environment Center (CQMA) - Nuclear and Energy Research Institute (IPEN), São Paulo, Brazil

ARTICLE INFO

Article history:
Received 29 September 2016
Received in revised form 23 December 2016
Accepted 21 March 2017
Available online 23 March 2017

1. Introduction

Tissue engineering is a multidisciplinary field which aims tissue regeneration, by using biomaterials [1]. Tissue regeneration (TR) techniques are increasingly used for the treatment of periodontal defects, reconstruction of lost, damaged and atrophied bone tissue, dental implant procedures or to preserve alveolar sockets after tooth extraction [2]. Generally, polymeric membranes used in TR are roughly divided into bioabsorbable and non-resorbable, where in both cases they should have the following properties: biocompatibility, maintenance in the implanting space, adaptation to the area of use, flexibility and optimal coverage of tissue defect [3,4].

Electrospinning is a manufacturing process used to obtain fibers with diameters in the range of micrometer to nanometer scale. This technique allows obtaining fibers with great potential for a variety of biomedical applications, such as scaffolds (three-dimensional porous structures), fiber mats for controlled drug delivery and guided tissue regeneration (GTR), adsorbent materials, among others [5,6]. Thus, there is a wide range of potential applications of such membranes in periodontology and oral implantology, since polymeric membranes can act as a barrier, which helps preventing epithelial tissue migration to the defective area, allowing sufficient time for bone regeneration, cementum and periodontal ligament [3]. Such membranes act in retaining the blood clot and providing a waterproof environment to the migration of unwanted cells, which may compromise bone repair [7]. Researches in the bioengineering field have developed several non-resorbable and resorbable membranes for use in GTR [8]. These developments were aimed to improve the limitations of non-resorbable classical barriers of expanded polytetrafluoroethylene (ePTFE),which has disadvantages such as the risk of premature implant removal and the necessity of a second surgical stage for implant removal [9]. To overcome some of these limitations, polymeric membranes PLGA/PGA have shown to be as efficient as ePTFE; however, its hydrolytic degradation associated with the reabsorption of part of the regenerated bone, can compromise the host response [10,11]. Collagen membranes appeared as a natural substitute that could promote tissue integration and transport of nutrients. However, the fast degradation by enzymatic activity of macrophages and polymorphonuclear leucocytes, substantially reduces the mechanical strength leading to membrane collapsing [8]. Therefore, in order to obtain suitable membranes to be used as a physical barrier, polymers used in tissue regeneration, PCL and PR, were studied and its biological behavior by means of a electrospun polymer blend was evaluated on a guided bone regeneration model.

* Corresponding author at: Department of Manufacturing and Materials Engineering,School of Mechanical Engineering, University of Campinas, Campinas. Rua Mendeleyev, 200, CEP 13083-860, Cidade Universitária "Zeferino Vaz" Barão Geraldo, Campinas, SP, Brazil.
E-mail addresses: tais_helenacs@yahoo.com.br (T.H.C. Salles), dsendyk@usp.br (D.I. Sendyk), natachakalline@hotmail.com (N.K. de Oliveira), daisy.machado@gmail.com (D. Machado), lancellottim@gmail.com (M. Lancellotti), mczdebon@usp.br (M.C.Z. Deboni), chang.kiang@gmail.com (C.T. Kiang), madavila@fem.unicamp.br (M.A. d'Ávila).

http://dx.doi.org/10.1016/j.msec.2017.03.190
0928-4931/

Table 1
Electrospinning parameters.

Parameter	PCL*	PCL/PR**
Flow rate (mL/h)	1	5
Voltage (kV)	15	20
Needle (mm)	0,55	0,7
Distance (cm)	10	20

Poly(ε-caprolactone) (PCL) is a biodegradable semicrystalline synthetic polymer with good biocompatibility and flexibility. It is a hydrophobic polymer with high mechanical strength and low cytotoxicity. PCL is approved by FDA for use as a biomaterial [12]. Biomedical applications of this polymer are diverse, such as drug controlled release and tissue engineering in epidermal, muscle, bone and cartilage tissues [13,14].

Poly(rotaxane) (PR) is a polymer with supramolecular topological architecture, with the inclusion of multiple cyclic molecules (e.g. α-cyclodextrins) in a linear polymer (e.g. polyethylene glycol, PEG), and the chain ends blocked with bulky groups (e.g. adamantanaminas) [15,16]. Cyclodextrins (CD) are cyclic oligosaccharides formed by D-glucose molecules bonded together via connections (α-1, 4) and are crystalline, homogeneous and non-hygroscopic. Its molecules have annular primary hydroxyl groups in the narrowest part of the cone, while secondary hydroxyl groups are at the widest part of the cone. Thus, the hydroxyl groups on the extremity make cyclodextrins hydrophilic and solvable in water [17]. This material has excellent elasticity and swelling properties, which is attractive for various applications in the biomedical field, such as in bioactive drug delivery system and biocompatible hydrogels [15,16,18,19].

In the present study, eletrospun PCL and PCL/PR blend fiber mats were obtained aiming future applications in tissue regeneration. To our knowledge, studies of electrospun PCL/PR blends aiming biomedical applications have not been reported previously in the literature.

The objective of this study was to obtain by electrospinning a nanofiber pure PCL and its blends of with polyrotaxane (PCL/Poly), to analyzed comparatively some of the micromorphological characteristics and the in vitro behavior of the pure fiber and its blend and to verify the effect of blend of PCL/PR in recovering a critical bone defect in vivo.

2. Materials and methods

2.1. Materials

PCL with molar mass of 80,000 g/mol (Sigma Aldrich), chloroform (Merck, Germany) and acetone (Synth-Brazil) were used as received. PR with molecular weight 496,000 g/mol and hydroxyl index of 71 mg KOH/g was gently supplied by UBE and this is a non-commercial grade.

Chloroform and acetone were mixed in different proportions by weight and polymer solutions were obtaining by adding PCL and PR (1:1). Solutions were magnetically stirred for 2 h at 23 °C and 150 rpm. All solutions was electrospun in the same day of preparation.

2.2. Electrospinning

The electrospinning system used in this study consisted of a 10 mL syringe and needles of 0.55 to 0.7 mm in diameter, an infusion pump (kdScientific, KDS-100 Model), a high voltage source (Testtech) and a grounded collector plate. Solutions were electrospun at 23 °C with voltages from 15 to 20 kV and flow rates from 1 to 5 mL/h. Table 1 shows the electrospinning parameters used in this work.

2.3. Characterization

The morphology of the electrospun membranes were evaluated by scanning electron microscopy (SEM) (Zeiss, Evoma-15). Samples were coated with gold using a sputter coater equipment (Bal-Tec, SCD-O5O). Fiber average diameters were determined from SEM images using ImageJ software, where diameters of 50 randomly chosen fibers from each sample were measured.

Contact angle of electrospun mats were measured in order to evaluate the hydrophilic character of PCL and PCL/PR blend. An optical microscope Hitachi with Axio s40 software V4.8.2.0 was used. Drops of the deionized water (5.0 μL) were placed on the surface of the sample using a pipette(Transferpette). All measurements were performed at

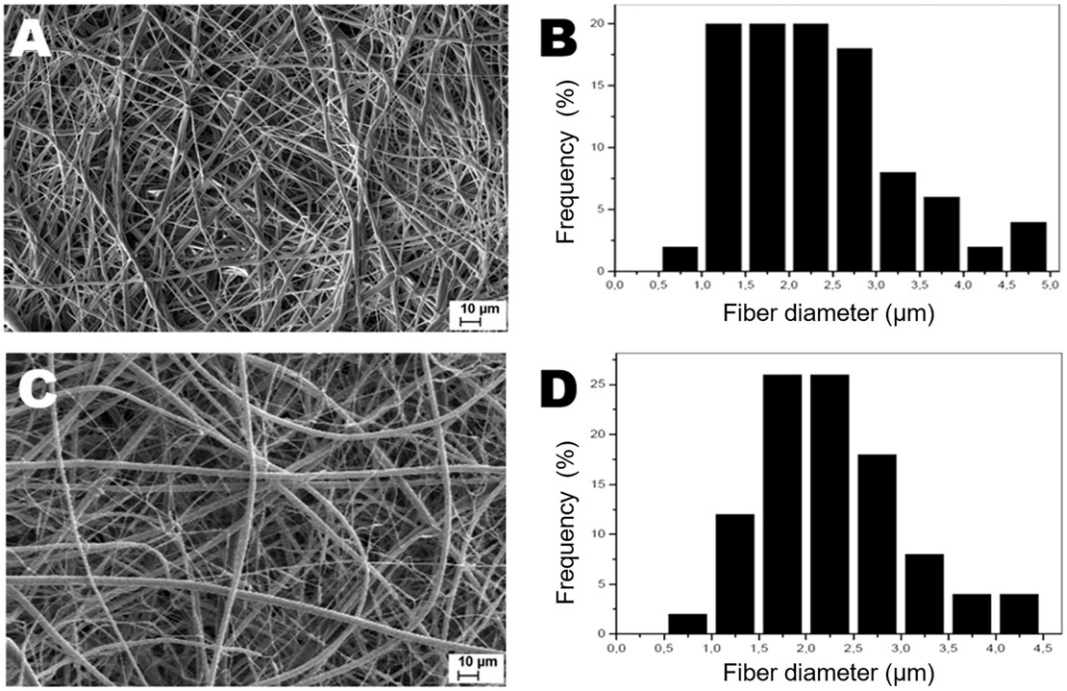

Fig. 1. Micrograph of electrospun fibers (A) PCL and (C) PCL/PR. Histogram of fiber diameter distributions (B) PCL and (D) PCL/PR.

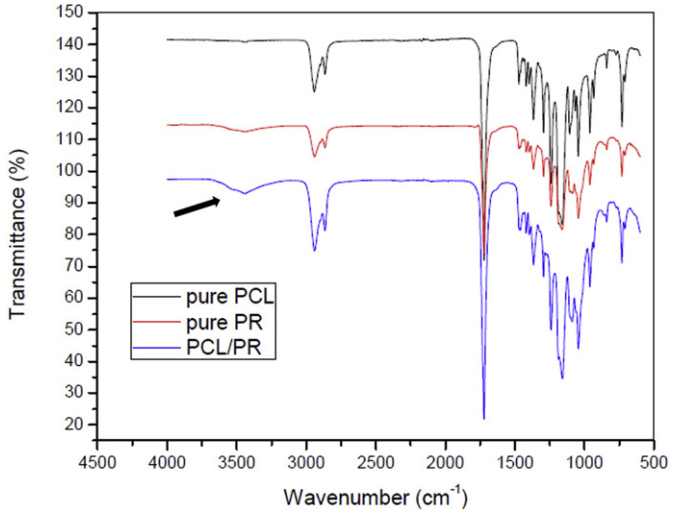

Fig. 2. FTIR spectra for a pure PCL, pure PR and blend PCL/PR. The arrow points to –OH peak at 3458 cm^{-1}.

25 ± 3 °C with relative humidity of 40 ± 4%. The contact angles were measured using ImageJ 1.47v with the plugin Drop Analysis (LB-ADSA) Three measurements were performed for each group of samples and average values and standard deviations were obtained.,. F-test of two sample variance ($P < 0.05$) was also performed in order to point out statistically significant differences between samples.

Fourier transform infrared-attenuated total reflectance spectroscopy (FTIR-ATR) was performed. The spectra was recorded at room temperature in a Perkin-Elmer Spectrum 65 Spectrometer in the 4000–600 cm^{-1} range. For FTIR analysis, blend samples of PCL/PR were prepared in the form of films.

2.4. In vitro tests

2.4.1. Cell culture

Non-cancerous NIH - 3T3 (fibroblast embryonary of *Mus musculus*, purchased from ATCC® CRL-1658™) established cell line were cultured in RPMI 1640 (Cultilab, Brazil) supplemented with 10% fetal bovine serum (FBS) (Crypion, Brazil) and 1% antibiotic (penicillin and streptomycin) (Cultilab, Brazil). Cells were plated in 75 cm^2 bottles at a density of 2×10^4 cells/mL and incubated at 37 °C under humid atmosphere with 5% CO_2. When cell culture achieved confluency of 75% of the culture flask subcultures were processed for cytotoxic tests.

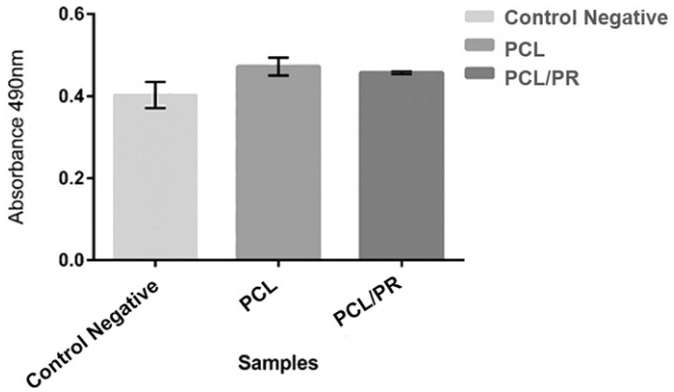

Fig. 3. Evaluation of cytotoxicity of biomaterials in BALB / c 3 T3 cells. The BALB/c 3 T3 cells were treated with different biomaterials for 24 h. The values were expressed as a percentage reduction of MTT compared the test control, where cells were not exposed to biomaterials. The experiment was realized 24-well microplate and the results represent averages and standard deviations of the experiment. * $P < 0.05$.

Table 2
Distribution of final sample in groups and experimental periods.

Group	7 days	14 days	21 days	42 days
PCL/PR	4	5	7	5
Control	5	5	5	5

2.4.2. Cytotoxic test

Cells were plated at a density of 6×10^4 cells/mL in 24 well plates already containing 13 mm diameter glass coverslips (control group) or dishes in the same diameter of the membrane of pure PCL or PCL/PR. They were subsequently incubated at 37 °C, 5% CO_2 for 24 h. After 24 h of incubation, the medium was removed, the wells were washed with phosphate buffered saline buffer (PBS) and serum-free medium containing thiazolyl blue tetrazolium bromide (MTT) solution (0.5 mg / mL) (Sigma Aldrich, USA) were added. After incubation for 3 h and 37 °C, the medium was carefully removed and added to 100 μL ethanol to solubilize the formazan. The plates were shaken for 5 min and the absorbance corresponding to each well was read on a digital spectophotometer ELx800 Absorbance Microplate Reader (Biotek, USA) in λ = 570 nm [13]. The measured absorbance at λ = 490 nm was normalized to % of control. These values were calculated by multiplying the absorbance of a treated well by 100 and dividing it by the average absorbance of control well, which was considered 100% [20,21].

2.5. In vivo procedures

All experimental procedures were performed in accordance with the International Care and Use of Laboratory Animals and were approved by the Institutional Ethic Committee for Animal Research (CEP FOUSP Nº. 20/2013).

Forty male *Rattus norvegicus, albinus,* Wistar rats (Experimental Animal Center, ICB, Biomedical Science Institute, São Paulo, Brazil), weighing about 200 to 250 g, underwent surgery under general anesthesia with intramuscular injection of 0.8 mg/kg body weight (bw) of ketamine hydrochloride (Dopalen®, Vetbrands, São Paulo, Brazil) and 0.3 mg/kg bw of xylazine hydrochloride. All animals also received antibiotic prophylaxis via intramuscular injection with 150,000 IU/Kg bw of benzathine benzylpenicillin (Roche Brazil, São Paulo, Brazil). Access to the calvaria of the animal was via a rectilinear incision in the skin of the middle area of the cranium, followed by a lateral division of the subcutaneous tissue, temporal muscle, and periosteum. The bone defect was made with a steel trephine drill (8 mm in diameter; SIN®, São Paulo, Brazil), which was adapted to a dental handpiece on the implant drill (600 Baby®, Driller, São Paulo, Brazil) at low speed. Defects were made under constant saline solution irrigation. Finally, the skin was sutured with 3–0 silk suture thread (Ethicon, Somerville, NJ, USA). After surgery, the animals were randomly divided into two groups. Defects in test group ($n = 20$) received a PCL/PR membrane covering. Defects in control group ($n = 20$) did not have coverage by any membrane and were filled just by blood clot. All animals were kept in individual

Table 3
Average values ± standard deviation of the measurements of the radiographic area of bone defects between groups and time period.

Group	Time period (days)	n	Average ± DP (pixel/mm^2)	(p)
PCL/PR	7	4	52,89 ± 2,05	**0.014**
Control		5	56,44 ± 1.31	
PCL/PR	14	5	52,72 ± 7,34	0.60
Control		5	54,55 ± 4,39	
PCL/PR	21	7	51,34 ± 3,56	0.37
Control		5	52,95 ± 3,06	
PCL/PR	42	5	46,63 ± 4,99	0.08
Control		5	53,20 ± 2,09	

Test of Kruskal-Wallis. Significance $p \leq 0{,}05$.

plastic cages with standard diet (Labina®, Purina, São Paulo, Brazil) and water ad libitum.

2.5.1. Euthanasia and specimen fixation

Five animals from each group per experimental period were euthanized in a CO_2 chamber 7, 14, 21, and 42 days after the operation. After euthanasia, the skulls were dissected and specimens including the whole defect region of the calvarias were immediately fixed in buffered 10% formalin for x-ray images and histological preparation procedures.

2.5.2. Preparation of specimens for X-ray and image analyses

Prior to laboratory processing for histological analysis, all of the surgical samples were X-rayed. The X-ray images were obtained on periapical dental film (Kodak Insight, Eastman Kodak Co., USA) using a dental X-ray (Timex 70E, Gnatus® São Paulo, Brazil). All of the radiographies were obtained in a standardized way, using a focal distance of 4.5 cm and an X-ray exposure time of 3.2 s. The X-ray films of all of the samples were developed together, following standardized criteria of time and temperature. The X-ray analysis were blinded to the group designations and consisted of measurement of the radiolucent bone defect area using ImageJ (NIH, Bethesda, Maryland, USA) manual drawing tool.

2.5.3. Histological preparation and analysis

To prepare the histology sections the specimens were soaked in a 10% EDTA pH 7.4 solution for 6 weeks for decalcification of the bone tissue. The defect area was sectioned exactly on the middle sagittal plane of calvaria, resulting in two parts to the wound: left and right sides. Each side was included in its own paraffin block. Next, four 4.5-μm-thick parasagittal sections were stained with hematoxylin and eosin.

The histological sections were accessed blindly by a pathologist using a conventional light microscope (DM5000, Leica Microsystems, Germany) in 2,5× of magnification objective. The histomorphologic aspects of bone repair focused mainly on presence of inflammatory infiltrate, granulation tissue, necrosis, newly formed vessels and new bone formation. The histomorphometric analysis was perform to quantify the area of new bone formation in random histological sections from both sides of the defect (right and left) in three distinct regions of the wound: two in the lateral border and one in the center of the defect. Images of each area of the histological section were digitized and transferred to a digital morphometry software (ImageJ, NIH). New bone trabeculae formation in the histological section was recognized and outlined using "hand free" tool available in the software in the three regions of the defect. The measurements were performed in four histological semi-serial sections of each side. The total new bone formation area of each side was the sum of the area obtained in each field. This value was then summed to those obtained from the other side. At the end, it was obtained the mean of the total new bone formation area for each group and experimental period.

3. Results

3.1. Electrospinning

Fig. 1 presents SEM images of electrospun PCL and PCL/PR membranes. It can be observed that both electrospun PCL (Fig. 1a) and PCL/PR (Fig. 1c) mats presented similar morphologies, characterized as a nonwoven mat, with high diameter dispersity. It can be seen that the mats are highly porous without the presence of defects, such as beads. The average fiber diameter of the PCL(Fig. 1b) and PCL/PR (Fig. 1d) were 2.5 (±0.88) μm and 2.3 (±0.82) μm, respectively; therefore the samples are not statistically different regarding the fiber diameter.

3.2. Contact angle

Contact angle of PCL and PCL/PR were 131,58° ± 0,74° and 108,45° ± 3,72°, respectively. This result shows that the presence of PR improved the hydrophylicity of the mat shown by an 18% decrease in the average contact angle. The average value for PCL was comparable to those reported by other authors, with values ranging from 118° ± 6 to 124° ± 3 [13,14,15].

3.3. Fourier transform infrared (FTIR) spectroscopy

The FTIR spectra of pure components and PCL / PR blend are shown in Fig. 2 Spectrum showed typical bands about PCL and PR. The peaks at 2927–2840 cm^{-1} (pure PCL) and 2939–2865 cm^{-1} (pure PR) were assigned to the stretching vibration of –CH 2, peaks at 1715 cm^{-1} (pure PCL) and 1717 cm^{-1} (pure PR) were assigned to the stretching

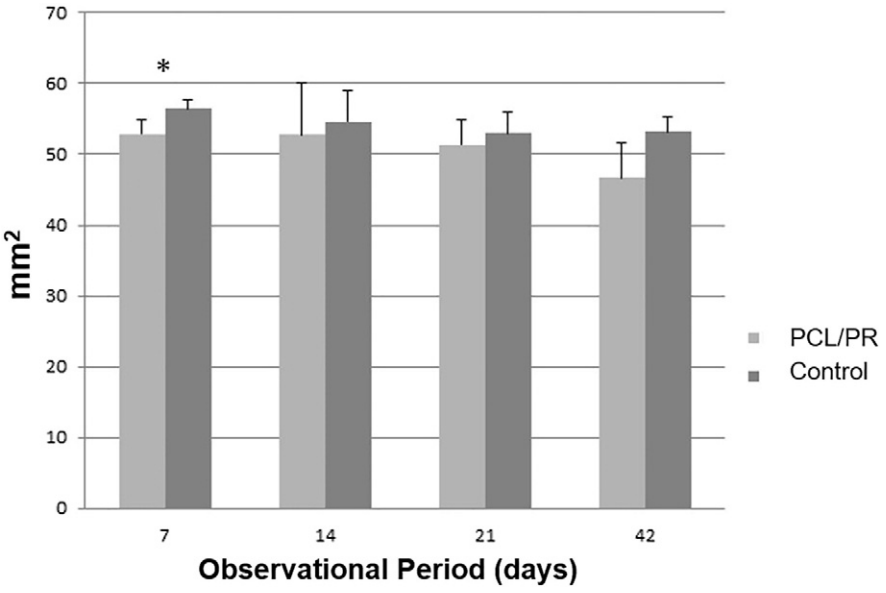

Fig. 4. The averages and standard deviation (mm^2) of the areas of the radiographic image of the defect in different experimental periods. Kruskal-Wallis and Mann-Whitney test. Significant when $p < 0.05$. A = statistically different in relation to collagen group in each experimental period.

vibration of –C = O bonds and peaks located at 1171 cm^{-1} (pure PCL) and 1161 (pure PR) corresponding to bands of alcohols CO [22,23]. In the pure PR, it is observed a peak of 3459 cm^{-1} characteristic of the hydroxyl group (OH) [23]. The change in the spectra of PCL upon the addition of PR to PCL reveals at –OH peak at 3458 cm −1 (Fig. 2 arrow).

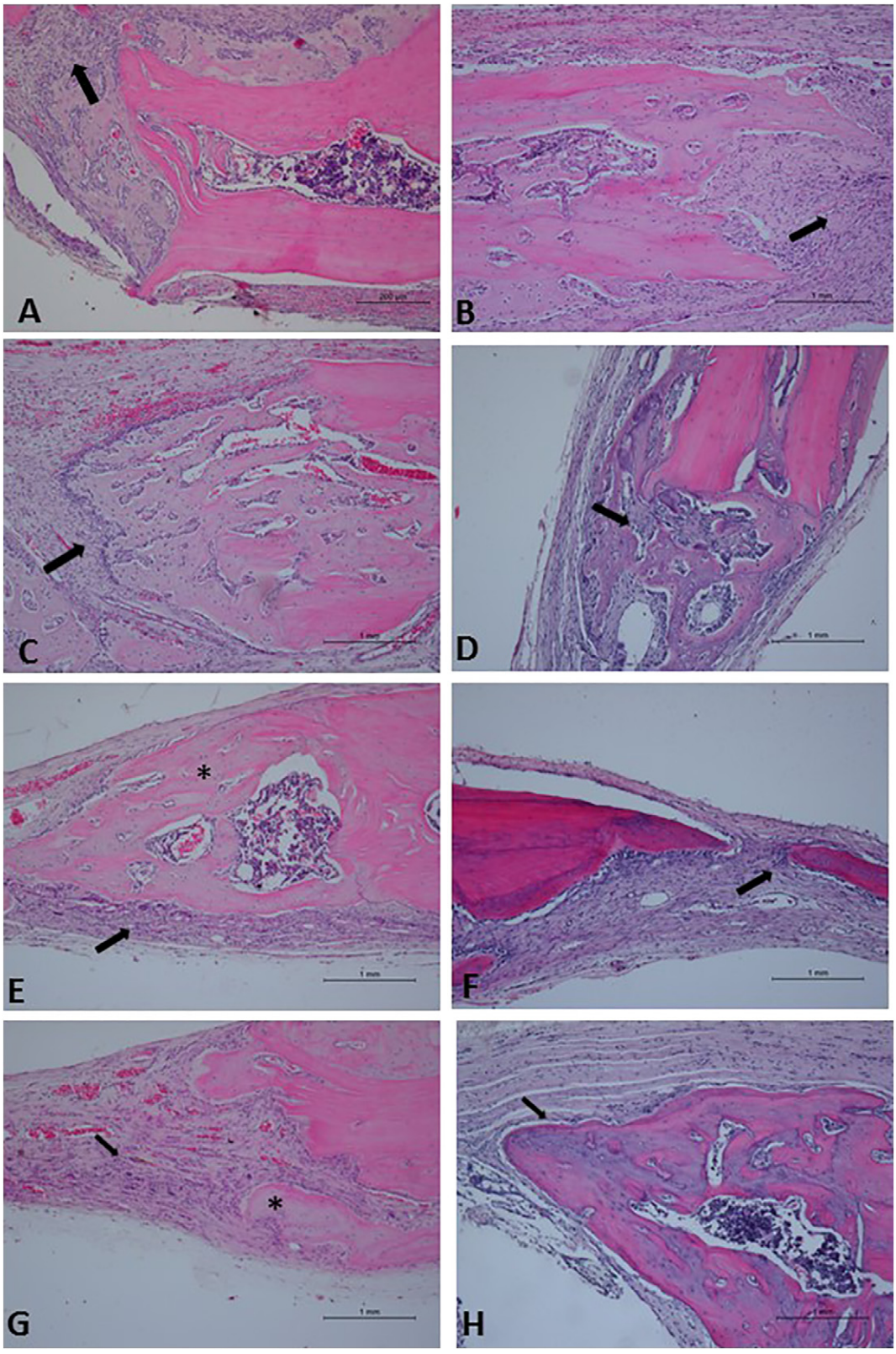

Fig. 5. Representative histology characteristics of the bone defect repair: Period of 7 days, A) PCL/poly group presented larger amount granulation tissue (arrow); B) control group, granulation tissue organization (arrow); period 14 days, C) PCL/poly group bone neoformation (arrow); D) control group in the bone formation area (arrow). Period of 21 days, E) PCL/poly group, showed formation of bone tissue (asterisk) and clusters of giant cells (arrow); F) control group, neoformed bone tissue (arrow). Period of 42 days, G) PCL/poly group, shows giant cell clusters (arrow) and bone neoformation (asterisk); H) Control group with bone neoformation (arrow). Hematoxylin and eosin, original magnification, objective 2.5×.

3.4. In vitro

Fig. 3 shows the mitochondrial activity assay results of the fibroblast cells murine (BALB / c 3 T3) in control and in the presence of biomaterials after 24 h. It can be observed that the biomaterials were not cytotoxic. The results indicate that the presence of PCL and PCL/PR has stimulated fibroblasts proliferation as compared to the control.

3.5. In vivo postoperative characteristics

From the 50 rats, eight (8) died in the next day of the experimental surgical procedure and one (1) at the time of anesthesia. The final sample consisted of 41 animals, distributed into three groups (Table 2).

During the perioperative period, the weight of the animals in all groups ranged from 240 g to 250 g, and on the day of euthanasia it ranged from 260 g to 320 g. None of the animals showed signs of infection in the surgical wound region. All wounds were cleaned and skin incision region did not present visible dehiscence or exhibition of the membrane to external environment.

3.5.1. Analysis of radiographic images

Table 3 shows a comparison between bone defect areas in both experimental groups. The average values and the corresponding standard deviations are presented in units of pixel/mm^2. Fig. 4 shows graphically the difference between the groups for the variable size of the bone defect image.

3.5.2. Histomorphological analysis

3.5.2.1. 7 day period. The PCL/PR group presented a neutrophilic infiltrate and lymphocyte more intense when compared to the control. The presence of osteoclasts is slightly more intense, but not significant in the control group. There was granulation tissue formation in the control group and similar results in necrosis and bone neoformation and giant cells (Fig. 5A and B).

3.5.2.2. 14 day period. The presence of giant cells was more intense in the PCL/PR group. The inflammatory process in the PCL/PR group remained moderate, with reduced intensity compared to the previous period. Areas of necrosis, granulation tissue and hemorrhage were similar in all groups as shown in Fig. 5C and D.

3.5.2.3. 21 day period. There was inflammation reduction in both groups. The presence of giant cells was more intense and significant in PCL/PR group ($p = 0.009$). Areas of necrosis, granulation tissue and hemorrhage were similar to control group and the membrane groups. There was an osteoclastic activity slightly larger in the control group (Fig. 5E and F).

3.5.2.4. 42 day period. The presence of giant cells was intense and significant in PCL/PR group. The bone neoformation was similar for both groups, however, there was a higher concentration of giant cells in the membrane group. The inflammatory infiltrate, areas of hemorrhage, necrosis and granulation tissue were similar (Fig. 5G and H).

3.5.3. Histomorphometric analysis

The average areas of bone neoformation measured by cutting three defect areas (anterior, central and posterior) in mm^2 are shown in Table 4. Fig. 6 shows graphically the differences in bone neoformation between groups according with the observation periods.

Table 4
Descriptive data in average ± standard deviation of the measurement bone neoformation area (μm^2), comparatively intergroup for each observation period.

Group	Time period(days)	n	Average ± SD (μm^2)	(p)
PCL/PR	7	4	23.886 ± 16.824	<**0.0001**
Control		4	20.52 ± 15.468	
PCL/PR	14	4	42.848 ± 17.204	0,1071
Control		4	37.81 ± 8.488	
PCL/PR	21	4	62.832 ± 21.174	0,0004
Control		4	43.278 ± 10.393	
PCL/PR	42	4	290.117 ± 121.742	0,2192
Control		4	335.864 ± 146.32	

Kruskal-Wallis Test. Significance $p \leq 0.05$.

4. Discussion

PCL and PCL/PR mats presented a broad fiber diameter distribution and the formation of pores and interconnects are supposed to promote good adhesion and proliferation of cells on the membrane. This ability to transport and allocate cells between in the porous fibrous structure has been discussed in the literature [24].

PCL is broadly used in biomedical applications, and the use of PR to form blends with PCL are interesting due to possibilities such as tuning mechanical and surface properties and even grafting active molecules of the hydroxyl group carried by cyclodextrins (α-CD), allowing functionalization of inherently inert polymers [7,25]. In this work, it was observed that PR improved the mat hydrophilicity, which may improve cell adhesion [26,27]. Hydrophilic scaffolds can absorb cell culture medium and when in receptor organic bed would absorb extracellular tissue liquids [28,29]. Hydrophilicity is a relevant characteristic because its guarantees nutrition distribution to the entirely scaffold surface and inner spaces essential to cell adhesion, proliferation and differentiation [29,30,31]. FTIR spectra peak showed that PR polymer contains hydroxyl groups in the narrowest part of the cone, what leaded to a more hydrophilic membrane. This was also observed from the angle contact assay for the polymeric membrane of PCL/PR.

Any biological test aims to verify the viability of a given biomaterials as well as propose improvements and customization for clinical applications. In this study, the membrane was used alone, since the goal was to test if the polymer could exert any effect on bone repair without interference from other bone substitutes or growth factors.

Both radiographic and histological images showed consistent and coherent results and complement each other. Radiographic images measurements showed that the decrease in the area corroborates with histologic findings. However, it should be noted that the radiographic image alone is a subjective and limited method to assess bone neoformation. Although coherent results between blinded image analysis and blinded histological findings reduced errors inherent to subjectivity. The radiograph shows a two-dimensional image, subject to distortion and overlapping of images. Microtomography and three-dimensional reconstruction would probably identify more precisely the standard of bone neoformation in that type of defect.

The histomorphological evaluation showed that bone neoformation in all groups was mature, organized and exhibited coalescent trabeculae. Between, 7 and 14 days, the collagen group presented a more intense inflammation, which reduces from 21 days and significant bone neoformation in all time periods. In 14, 21 and 42 days, the PCL/PR group presented an intense activity of giant cells, suggesting a foreign body reaction, and a further discussion is presented below.

In all of our experimental periods, remnants of membranes were found, what is in agreement with the literature, where the exogenous material could be observed in various evaluation periods, as in Polimeni [32] study that showed that PLA devices, exhibited a substantial amount of residual biomaterial in the periods of 3, 5, 7 e 12 months. In that study, the PLA device remained intact over the 12-month healing interval, signs of bioresorption were present, but they were confined to the periphery of the device. Moreover, histological analysis here, allows us to observe that bone formation occurred in a centripetal form, that is, from the edges to the center of the wound. It is interesting to note that, despite a higher bone neoformation after 42 days, bone formation was greater between 7

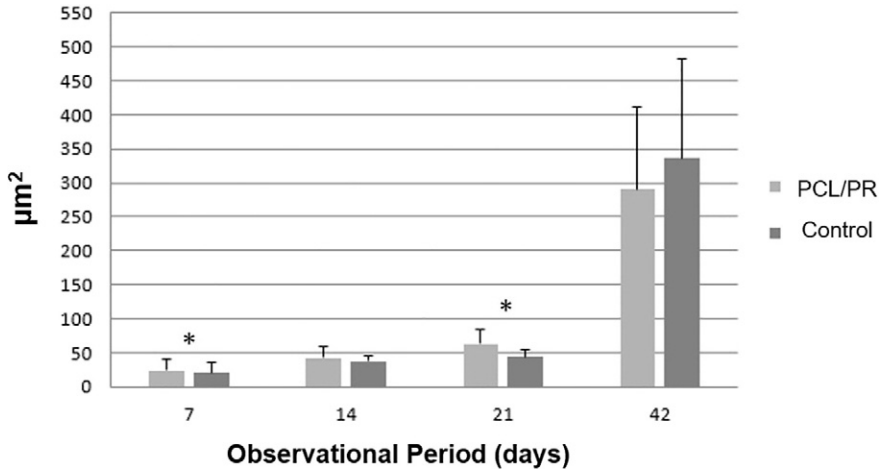

Fig. 6. Distribution of average and standard deviation of the total areas of new bone neoformation in µm^2. Kruskal-Wallis and Mann-Whitney test. Significant at $p < 0.05$. A = statistically different relative to collagen group in each experimental period.

and 14 days than those between 21 and 42 days, showing that in a critical defect, bone growth tends to stabilize.

We found that the comparative data, between the control and PCL/PR groups were very close, and therefore, the PCL/PR membrane did not promote an expressive guided bone regeneration. Moreover, we note that giant cell clusters were found more intensely in the PCL/PR group. Also, the permanence of giant cells in a late stage of repair could be possible due to an individualized response of animal species to the type of polymer used. The porosity of the membrane has probably influenced the chronic inflammatory response. In a first moment, this reaction to the foreign body could be considered as a negative factor for the biocompatibility effect of this membrane. However, some authors [33] have shown that the role of the foreign body reaction to biomaterials should be reconsidered, since the presence of giant cells with specific histochemical characteristics could be related to a stimulus for vascular tissue formation. Although, immunoreaction to vascular grown factors was not tested here, we observed that the presence of PCL/PR membrane seemed to have increased the presence of vessels. Immunohistochemical markers could confirm this hypothesis.

From our knowledge, the scientific literature about the use of electrospun mats of a synthetic polymer of the system PCL/PR for purposes of tissue engineering is nonexistent. Bioengineering adopts three strategies to create new organic tissues: firstly, the presence of cells, particularly stem cells, that could be characterized as differentiated cells to suitable tissue, secondly, specific grown factors must be presented to stimulate cells to proper differentiation and finally, the biocompatible scaffold to role as a structure, that will sustain and maintain viable cells to be transferred to a reception bed to form a new tissue [34]. The poly ε-caprolactone/poly(rotaxano) blend showed biocompatibility in vitro, revealing promising aspects to be functionalized by stem cells with potential to be used as bioactive biomaterials for bone tissue bioengineering. The potential of functionalizing this biomaterial with stem cells has been investigated by our group with promising results [35].

Geometry distribution of this polymeric blend fibers showed that cells have space, and porous interconnectivity to able cell proliferation and differentiation, although, other in vitro specific tests must be carry out to confirm this.

One might consider that electrospinning method used here is limited to the manufacture of patterned scaffolds, however, probably it will be possible to produce commercially standardized structures employing currently computational tridimensional printing. Thus, the original data obtained here should not discourage bioengineering, but stimulate further studies in order to improve and to understand the properties of such biomaterials.

The proposed model of PCL/PR membrane by electrospinning did not demonstrate effective performance for guided bone regeneration therapy in large bone defects when used alone. However, since it did not present cytotoxicity, and improvements regarding standardization in its production and morphological characteristics are possible, it could lead to studies of this material as a bioactive scaffold or as a carrier for other substances that promote guided bone regeneration.

5. Conclusion

Electrospun PCL and PCL/PR membranes were successfully produced. By adding PR, the hydrophilicity of the fiber mats increased when compared with the pure PCL, and both presented biocompatibility and favored in vitro cell growth after 24 h. For the case of in vivo tests, PCL/PR membranes has promoted an intense activity of giant cells, suggesting a foreign body reaction; however, in vivo behavior was stable and did not increase the critical defect area and its performance was comparable to the control group. Under the limits of this study, PCL/PR electrospun membranes demonstrated that it was not cytotoxic in a rapid test of 24 h; however this material did not enhance repair in a bone critical-sized defect.

Conflict of interest

Authors disclosure any conflicts of interest.

Acknowledgements

The authors thank the financial support from CNPq - Conselho Nacional de Desenvolvimento Científico e Tecnológico (308660/2015-3 and 401297/2014-4), CAPES – Coordenação de Aperfeiçoamento de Pessoal de Nível Superior (1199553) and FAPESP 15/15055-0 (Fundação de Amparo à Pesquisa do Estado de São Paulo).

References

[1] A. Kulkarni, V.A. Bambole, P.A. Mahanwar, Electrospinning of polymers, their modeling and applications, Polym.-Plast. Technol. Eng. 49 (2010) 427–441, http://dx.doi.org/10.1080/03602550903414019.
[2] M.N. Sela, M.N. Sela, Enzymatic Degradation of Collagen-Guided Tissue Regeneration Membranes by Periodontal Bacteria, 1995 263–268.
[3] J. Wang, L. Wang, Z. Zhou, H. Lai, P. Xu, L. Liao, et al., Biodegradable Polymer Membranes Applied in Guided Bone/Tissue Regeneration: A Review, 2016 1–20, http://dx.doi.org/10.3390/polym8040115.
[4] J. Xue, R. Shi, Y. Niu, M. Gong, P. Coates, A. Crawford, et al., Fabrication of drug-loaded anti-infective guided tissue regeneration membrane with adjustable biodegradation property, Colloids Surf. B: Biointerfaces 135 (2015) 846–854.

[5] K. Garg, G.L. Bowlin, Electrospinning jets and nanofibrous structures Electrospinning jets and nanofibrous structures, Biomicrofluidics 13403 (2014)http://dx.doi.org/10.1063/1.3567097.
[6] B. Ghorani, N. Tucker, Food hydrocolloids fundamentals of electrospinning as a novel delivery vehicle for bioactive compounds in food nanotechnology, Food Hydrocoll. 51 (2015) 227–240, http://dx.doi.org/10.1016/j.foodhyd.2015.05.024.
[7] M. Oster, A. Hébraud, S. Gallet, A. Lapp, E. Pollet, L. Avérous, et al., Star-pseudopolyrotaxane organized in nanoplatelets for poly (ε-caprolactone)-based nanofi brous scaffolds with enhanced surface reactivity, Macromol. Rapid Commun. (n.d.) 292–297.
[8] B.M. Annen, C.F. Ramel, C. Hans, F. Hämmerle, R.E. Jung, B.M. Annen, et al., Use of a new cross-linked collagen membrane for the treatment of peri-implant dehiscence defects: a randomised controlled double-blinded clinical trial, Eur J Oral Implantol 4 (2011) 87–100.
[9] Nyman,1982.pdf, (n.d.).
[10] Hurzeler,1997.pdf, (n.d.).
[11] B. Al-nawas, M.O. Klein, H. Terheyden, Use of a new cross-linked collagen membrane for the treatment of dehiscence-type defects at titanium implants: a prospective , randomized- controlled double-blinded clinical multicenter study, Clin. Oral Implants Res. (2009) 742–749, http://dx.doi.org/10.1111/j.1600-0501.2008.01689.x.
[12] M.A. Woodruff, D.W. Hutmacher, Progress in polymer science the return of a forgotten polymer, Polycaprolactone in the 21st Century, 35, 2010, pp. 1217–1256, http://dx.doi.org/10.1016/j.progpolymsci.2010.04.002.
[13] S. Gautam, A. Kumar, N. Chandra, Fabrication and characterization of PCL/gelatin composite nano fi brous scaffold for tissue engineering applications by electrospinning method, Mater. Sci. Eng. C 33 (2013) 1228–1235, http://dx.doi.org/10.1016/j.msec.2012.12.015.
[14] Z.X. Meng, W. Zheng, L. Li, Y.F. Zheng, Fabrication and characterization of three-dimensional nanofiber membrance of PCL – MWCNTs by electrospinning, Mater. Sci. Eng. C 30 (2010) 1014–1021, http://dx.doi.org/10.1016/j.msec.2010.05.003.
[15] T.E. Lipatova, L.F. Kosyanchuk, Y.P. Gomza, V.V. Shilov, Y.S. Lipatov, Polymeric rotaxanes, Dokl. Akad. Nauk 263 (1982) 1379–1982 Chem. 10.1021/cr9000622.
[16] Y. Okumura, K. Ito, The Polyrotaxane Gel: A Topological Gel by Figure-of-Eight Cross-links, Adv. Mater. 13 (No. 7) (2001) April 4.
[17] P. Wang, J. Wang, L. Ye, A. Zhang, Z. Feng, Poly (ε-caprolactone) end-capped with poly (N-isopropylacrylamide)s, Polymer 53 (2012) 2361–2368, http://dx.doi.org/10.1016/j.polymer.2012.03.060.
[18] J. Araki, K. Ito, Recent advances in the preparation of cyclodextrin-based polyrotaxanes their applications to soft materials, Soft Matter 3 (2007) 1456–1473, http://dx.doi.org/10.1039/B705688E.
[19] X. Gong, R. Jiang, X. Liao, H. Xie, X. Ma, C. Gao, Synthesis, characterization and in vitro evaluation of a series of novel polyrotaxane-based delivery system for artesunate, Carbohydr. Res. 412 (2015) 7–14, http://dx.doi.org/10.1016/j.carres.2015.04.021.
[20] T. Mosmann, Rapid Colorimetric Assay for Cellular Growth and Survival: Application to Proliferation and Cytotoxicity Assays, J. Immunol. Methods 65 (1983) 55–63.
[21] M.P. Prabhakaran, J.R. Venugopal, T.T. Chyan, L.B. Hai, C.K. Chan, A.Y. LIM, S. Ramakrishna, Electrospun Biocomposite Nanofibrous Scaffolds for Neural Tissue Engineering, Tissue Eng. Part A Vol 14 (Number 11) (2008)http://dx.doi.org/10.1089/ten.tea.2007.0393.
[22] G. Ciardelli, V. Chiono, G. Vozzi, M. Pracella, A. Ahluwalia, N. Barbani, et al., Blends of poly-(epsilon-caprolactone) and polysaccharides in tissue engineering applications, Biomacromolecules 6 (2005) 1961–1976, http://dx.doi.org/10.1021/bm0500805.
[23] A.K. Bassi, J.E. Gough, M. Zakikhani, S. Downes, The chemical and physical properties of poly(ε-caprolactone) scaffolds functionalised with poly(vinyl phosphonic acid-co-acrylic acid), J. Tissue Eng. 615328 (2011)http://dx.doi.org/10.4061/2011/615328.
[24] X. Zhu, W. Cui, X. Li, Y. Jin, Electrospun Fibrous Mats with High Porosity as Potential, (2008) 1795–1801.
[25] Y.K. Joung, H.D. Park, N. Yui, K.D. Park, Supramolecular Structures with Cyclodextrins for Biomedical Applications, Biomaterials Res. 11 (4) (2007) 162–169.
[26] Y. Wan, J. Yang, J. Yang, J. Bei, S. Wang, Cell adhesion on gaseous plasma modified poly- (L-lactide) surface under shear stress field. Biomaterials 24 (2003) 3757–3764, http://dx.doi.org/10.1016/S0142-9612(03)00251-5.
[27] K. Webb, V. Hlady, P.A. Tresco, NIH Public Access 41 (2009) 422–430.
[28] Y. Zhang, W. Fan, Z. Ma, C. Wu, W. Fang, G. Liu, et al., The effects of pore architecture in silk fibroin scaffolds on the growth and differentiation of mesenchymal stem cells expressing BMP7, Acta Biomater. 6 (8) (2010) 3021–3028.
[29] X. Zheng, F. Yang, S. Wang, S. Lu, W. Zhang, S. Liu, et al., Fabrication and cell affinity of biomimetic structured PLGA/articular cartilage ECM composite scaffold, J. Mater. Sci. Mater. Med. 22 (3) (2011) 693–704.
[30] Y. Zhu, T. Liu, K. Song, B. Jiang, X. Ma, Z. Cui, Collagen-chitosan polymer as a scaffold for the proliferation of human adipose tissue-derived stem cells, Journal of Materials Science-Materials in Medicine 20 (3) (2009) 799–808.
[31] H. Seyednejad, D. Gawlitta, W.J. Dhert, C.F. van Nostrum, T. Vermonden, W.E. Hennink, Preparation and characterization of a three-dimensional printed scaffold based on a functionalized polyester for bone tissue engineering applications, Acta Biomater. 7 (5) (2011) 1999–2006.
[32] G. Polimeni, K. Koo, G.A. Pringle, A. Agelan, F.F. Safadi, U.M.E. Wikesjö, Histopathological Observations of a Polylactic Acid-Based Device Intended for Guided Bone/Tissue Regeneration, (n.d.) 99–105. doi:10.1111/j.1708-8208.2007.00067.x.
[33] S. Ghanaati, M. Barbeck, C. Orth, I. Willershausen, B.W. Thimm, C. Hoffmann, et al., Influence of b-tricalcium phosphate granule size and morphology on tissue reaction in vivo, Acta Biomater. 6 (2010) 4476–4487, http://dx.doi.org/10.1016/j.actbio.2010.07.006.
[34] S. Changotade, G. Radu Bostan, A. Consalus, F. Poirier, J. Peltzer, J.J. Lataillade, et al., Preliminary in vitro assessment of stem cell compatibility with cross-linked poly(ε-caprolactone urethane) scaffolds designed through high internal phase emulsions, Stem Cells Int. 2015 (2015) 283796, http://dx.doi.org/10.1155/2015/283796 (Epub 2015 May 28).
[35] M. Deboni, Effect of membranes of nanofibrous poly(e-caprolactone)/poly(rotaxane) electrospinning blends on the viability of human dental pulp stem cells basic research, Clin. Oral Implants Res. 27 (7) (2016)http://dx.doi.org/10.1111/clr.6_12958.